Electronic Supplementary Material (ESI) for Nanoscale.
This journal is © The Royal Society of Chemistry 2014

# Supporting Information

# Nitrogen-doped graphdiyne as metal-free catalyst for high-performance oxygen reduction reaction

**Rongji Liu[a,b], Huibiao Liu[c], Yuliang Li[c], Yuanping Yi[c], Xinke Shang[a,b], Shuangshuang Zhang[a,b], Xuelian Yu[a], Suojiang Zhang[a], Hongbin Cao[a] and Guangjin Zhang*[a]**

[a]*Key laboratory of Green Process and Engineering, Institute of Process Engineering, Chinese Academy of Sciences, 100190, Beijing, China.*
*Email: zhanggj@home.ipe.ac.cn*

[b]*University of Chinese Academy of Sciences, 100049, Beijing, China.*

[c]*CAS Key Laboratory of Organic Solids, Beijing National Laboratory for Molecular Sciences (BNLMS), Institute of Chemistry, Chinese Academy of Sciences, 100190, Beijing, China*

## (1) Electrocatalytic oxygen reduction reaction

The reduction of $O_2$ in alkaline solutions can be proceeded by the following two overall pathways:[S1, S2]

(1) Direct $O_2$ reduction to $OH^-$ ions, what is called direct four-electron pathway (I):

$$O_2+2H_2O+4e^-\rightarrow 4OH^- \qquad \text{(I)}$$

(2) Or $O_2$ reduction to $HO_2^-$ ions, what is called two-electron pathway (II):

$$O_2+H_2O+2e^-\rightarrow HO_2^-+OH^- \qquad \text{(II)}$$

followed by either the further two-electron reduction of peroxide ion to $OH^-$ ions (III):

$$HO_2^-+H_2O+2e^-\rightarrow 3OH^- \qquad \text{(III)}$$

or the decomposition reaction (IV):

$$2HO_2^-\rightarrow 2OH^-+O_2 \qquad \text{(IV)}$$

In order to establish the extent to which each of the two pathways mentioned above is involved at a particular electrode surface, the RDE experiments (LSV experiments) were performed and the Koutecky–Levich equation was used to further study the catalysis of the prepared nanohybrids for the kinetics of ORR. For a typical LSV experiment, the working electrode was scanned cathodically at a rate of 5 mV $s^{-1}$ with varying rotating speed from 400 rpm to 1600 rpm. Koutecky–Levich plots obtained from the LSV curves ($J^{-1}$ vs. $\omega^{-0.5}$) were analyzed at various electrode potentials. The slopes of their best linear fit lines were used to calculate the transferred electron number (n) per oxygen molecule involved in the oxygen reduction at each of the electrodes on the basis of the Koutecky-Levich equation: [S3]

$$\frac{1}{\mathrm{j}} = \frac{1}{\mathrm{j_k}} + \frac{1}{B\omega^{0.5}}$$

where $j$ is the measured current density at a given potential, $j_\mathrm{k}$ is the kinetic current density, and ω is the electrode rotating rate. Therefore, $1/B$ is the calculated slope and its unit is $\mathrm{mA^{-1}\ cm^2\ rpm^{0.5}}$. $B$ could be determined from the slope of Koutecky-Levich plots based on the Levich equation as follows: [S4]

$$B = 0.2nF(D_{O_2})^{2/3} v^{-1/6} C_{O_2}$$

where $n$ represents the number of electrons transferred per oxygen molecule, $F$ is the Faraday constant ($F = 96485\ \mathrm{C\ mol^{-1}}$), $D_{O_2}$ is the diffusion coefficient of $O_2$ in 0.1 M KOH ($1.9 \times 10^{-5}\ \mathrm{cm^2\ s^{-1}}$), $v$ is the kinetic viscosity ($0.01\ \mathrm{cm^2\ s^{-1}}$), and $C_{O_2}$ is the bulk concentration of $O_2$ ($1.2\times10^{-6}\ \mathrm{mol\ cm^{-3}}$). The constant 0.2 is adopted when the rotation speed is expressed in rpm.[S4] The numbers of electrons transferred for ORR on each electrode calculated from the slopes of the Koutecky–Levich plots at various potentials are shown in Table S2.

The RRDE technique is another efficient method to estimate the electron transfer number (n), in which the peroxide species produced at the disk electrode were detected by the ring electrode. The disk electrode was scanned cathodically with a rotation speed of 1600 rpm at a scan rate of 10 mV $\mathrm{s^{-1}}$, and the ring potential was constant at 0.5 V vs. Ag/AgCl. The % $HO_2^-$ and n were calculated from the ratio of the ring current ($I_r$) and the disk current ($I_d$) following the equations given below: [S5]

$$\%HO_2^- = 200 \times \frac{I_r / N}{I_d + I_r / N}$$

$$n = 4 \times \frac{I_d}{I_d + {I_r}/{N}}$$

where N is current collection efficiency of the Pt ring (0.37).

## References:

S1 E. Yeager, *J. Mol. Catal.*, 1986, **38**, 5-25.
S2 J. J. Han, N. Li and T. Y. Zhang, *J. Power Sources*, 2009, **193**, 885-889.

S3 L. T. Qu, Y. Liu, J. B. Baek and L. M. Dai, *ACS Nano*, 2010, **4**, 1321-1326.

S4 S. Y. Wang, D. S. Yu and L. M. Dai, *J. Am. Chem. Soc.*, 2011, **133**, 5182-5185.

S5 H. Tang, H. Yin, J. Wang, N. Yang, D. Wang and Z. Tang, *Angew. Chem. Int. Ed.*, 2013, **52**, 5585 -5589.

## Supplementary data (Tables and Figures)

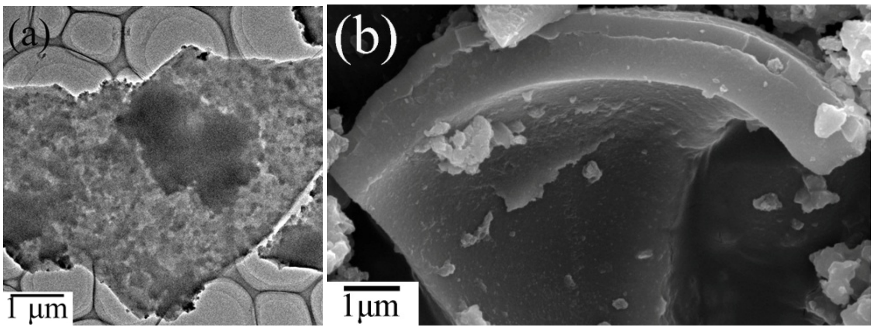

**Fig. S1** TEM (a) and FESEM (b) images of the prepared GD film.

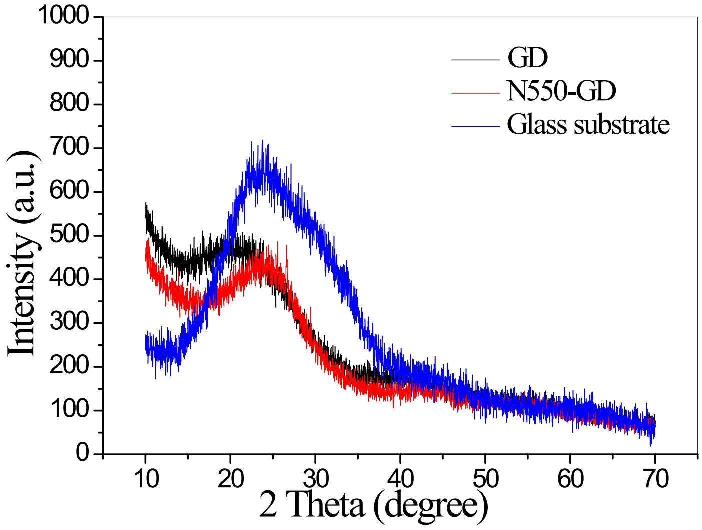

**Fig. S2** Powder XRD analysis of the prepared GD and N 550-GD powder, the XRD analysis of the blank glass substrate has been added for comparison .

**Table S1.** DFT-calculated N 1s binding energies (eV) for the N-doped GD.

| Molecule | N 1s alpha orbital | N 1s beta orbital |
|---|---|---|
| G3a | 392.8 | 392.8 |
| G3b | 394.3 | 394.3 |
| G3c | 392.2 | 392.1 |
| G3d | 390.5 | 390.5 |
| G4a | 392.9 | 392.9 |
| G4b | 394.4 | 394.4 |
| G4c | 392.3 | 392.2 |
| G4d | 390.4 | 390.4 |

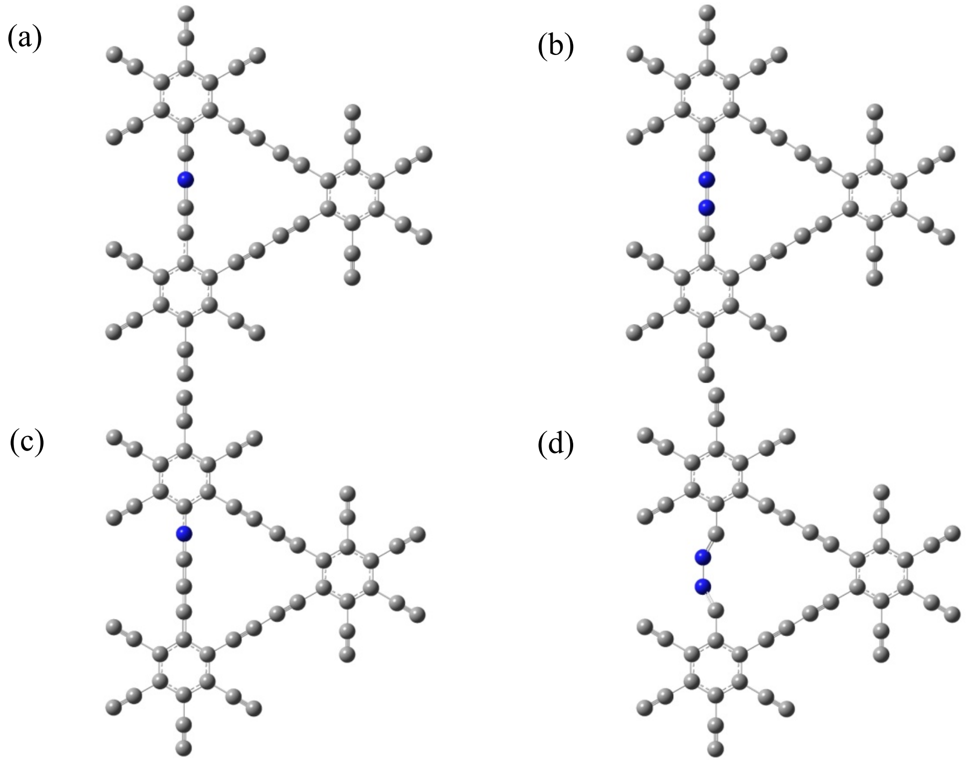

**Fig. S3** The models of N-doped GD (containing 3 units) in DFT calculations. (a) GD3a, (b) GD3b, (c) GD3c and (d) GD3d.

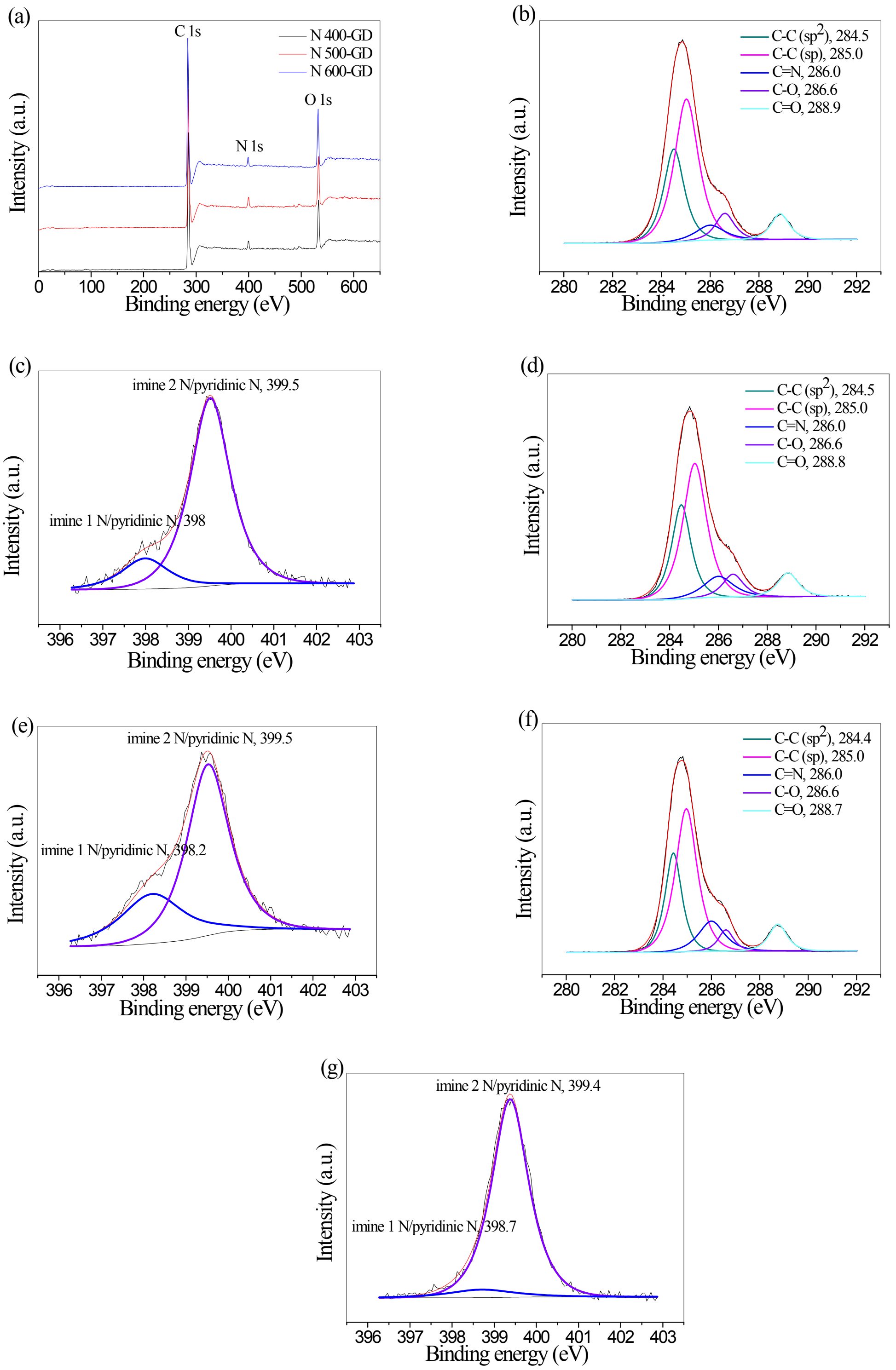

**Fig. S4** (a) XPS spectrums (survey) of N 400-GD, N 500-GD and N 600-GD. (b) and (c) are XPS C 1s and XPS N 1s spectrums of N 400-GD, respectively. (d) and (e) are XPS C 1s and XPS N 1s spectrums of N 500-GD, respectively. (f) and (g) are XPS C 1s and XPS N 1s spectrums of N 600-GD, respectively.

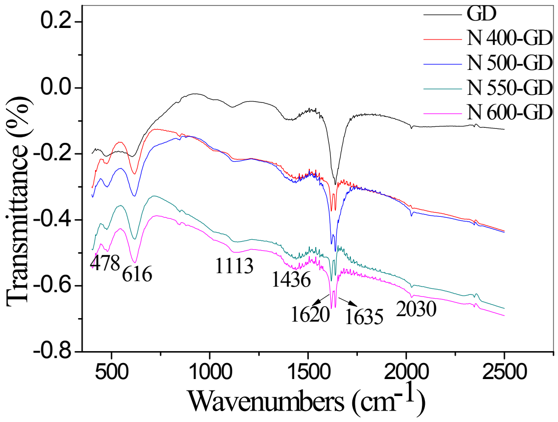

**Fig. S5** FT-IR spectrums of GD, N 400-GD, N 500-GD, N 550-GD and N 600-GD.

**Table S2.** The numbers of electrons transferred for ORR on the electrodes calculated from the slopes of the Koutecky–Levich plots at various potentials.

| Potentials | GD | N 400-GD | N 500-GD | N 550-GD | N 600-GD |
|---|---|---|---|---|---|
| 0.65 V vs. RHE | 3.49 | 3.13 | 3.43 | 3.71 | 4.24 |
| 0.55 V vs. RHE | 2.32 | 3.00 | 3.54 | 3.74 | 3.85 |
| 0.45 V vs. RHE | 2.40 | 3.15 | 3.61 | 3.77 | 3.74 |
| 0.35 V vs. RHE | 2.55 | 3.23 | 3.59 | 3.84 | 3.66 |
| 0.25 V vs. RHE | 2.73 | 3.30 | 3.66 | 3.81 | 3.63 |
| 0.15 V vs. RHE | 2.90 | 3.32 | 3.66 | 3.80 | 3.66 |
| 0.05 V vs. RHE | 3.06 | 3.35 | 3.68 | 3.78 | 3.67 |

**Table S3.** The kinetic-limiting current density ($j_k$, mA cm$^{-2}$) for ORR on the electrodes calculated from the intercepts of the Koutecky–Levich plots at various potentials.

| Potentials | GD | N 400-GD | N 500-GD | N 550-GD | N 600-GD |
|---|---|---|---|---|---|
| 0.65 V vs. RHE | 1.04 | 2.14 | 4.35 | 3.99 | 1.60 |
| 0.55 V vs. RHE | 4.39 | 4.84 | 7.58 | 7.24 | 3.72 |
| 0.45 V vs. RHE | 6.36 | 6.59 | 9.87 | 10.27 | 5.80 |
| 0.35 V vs. RHE | 6.95 | 7.74 | 11.87 | 11.99 | 7.54 |
| 0.25 V vs. RHE | 7.39 | 8.99 | 13.12 | 14.88 | 9.13 |
| 0.15 V vs. RHE | 8.21 | 10.99 | 15.26 | 17.98 | 10.88 |
| 0.05 V vs. RHE | 9.23 | 12.80 | 16.97 | 21.82 | 12.96 |

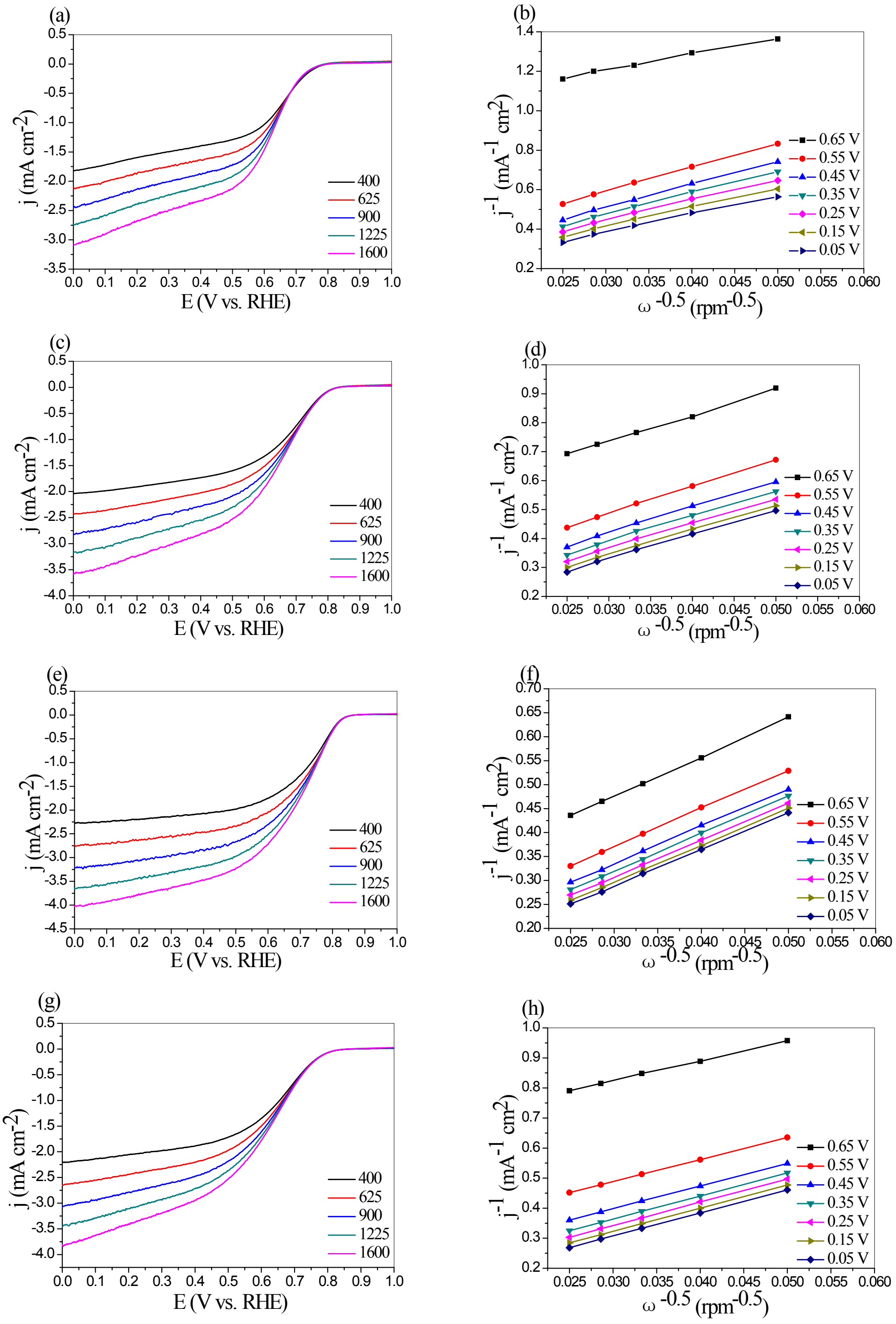

**Fig. S6** (a), (c), (e) and (g) are LSV curves of ORR at various rotation rates at GD, N 400-GD, N 500-GD and N 600-GD modified GC electrode respectively in $O_2$-saturated 0.1 M KOH solution at a scan rate of 10 mV s$^{-1}$. (b), (d), (f) and (h) are Koutecky-Levich plots for GD, N 400-GD, N 500-GD and N 600-GD obtained from the data in (a), (c), (e) and (g) respectively at various potentials.

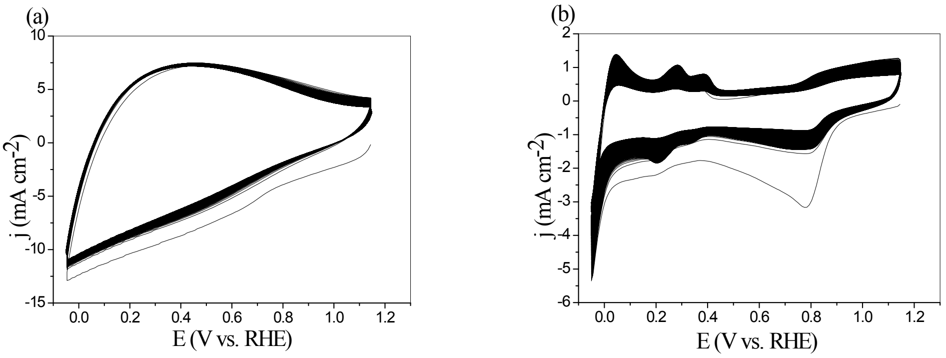

**Fig. S7** Continuous 6000 CV cycles of (a) N 550-GD and (b) Pt/C modified GC electrode in $O_2$ saturated 0.1 M KOH solution, scan rate was 200 mV $s^{-1}$.

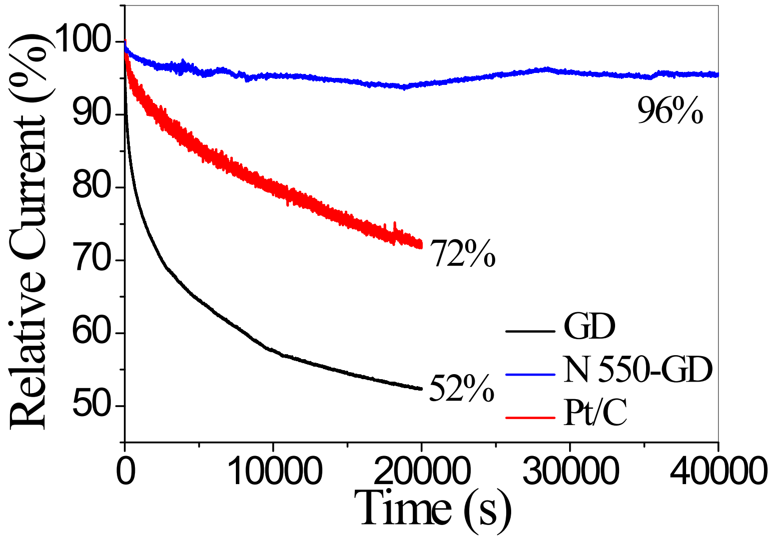

**Fig. S8** Current–time (i–t) chronoamperometric response of GD, N 550-GD and Pt/C modified GC RDE at 0.65 V vs. RHE in $O_2$-saturated 0.1 M KOH solution.

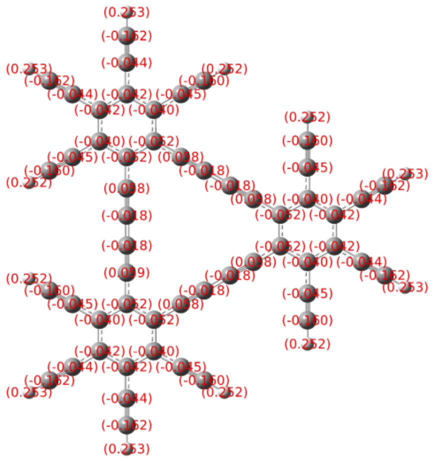
GD3

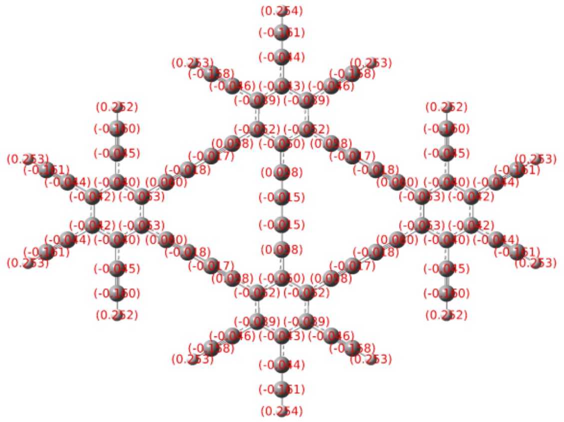
GD4

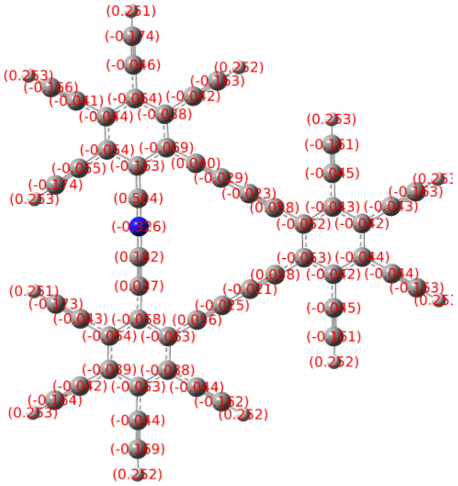
GD3a

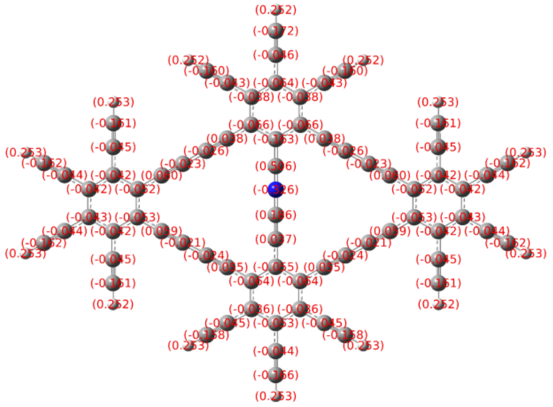
GD4a

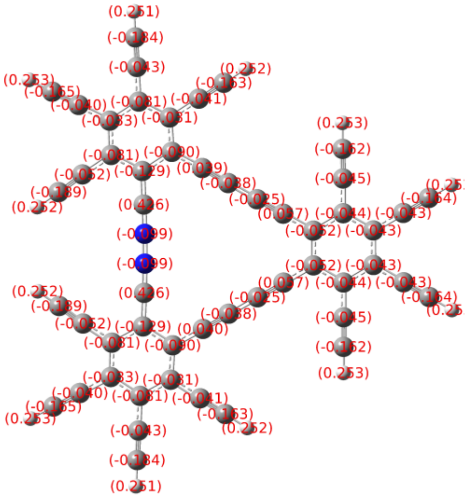
GD3b

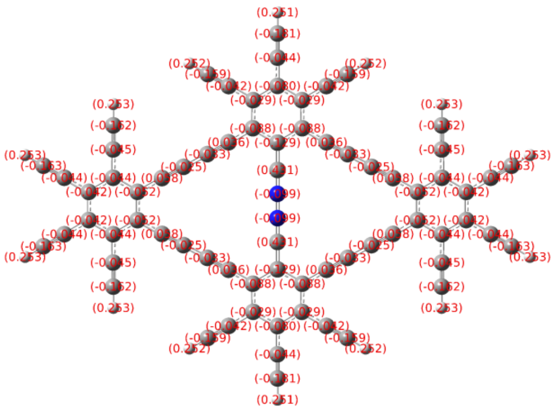
GD4b

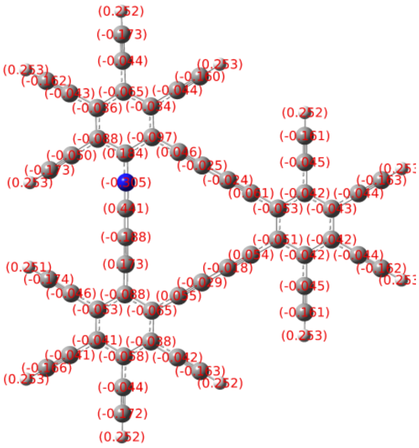

GD3c

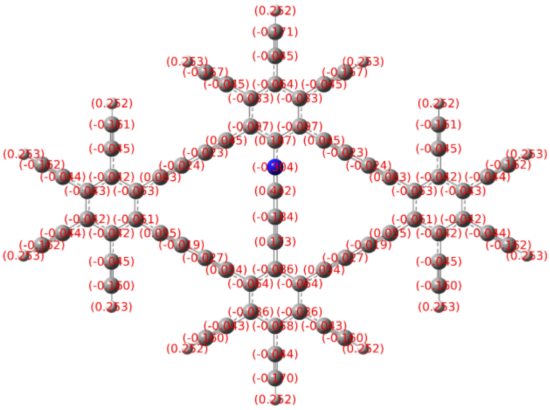

GD4c

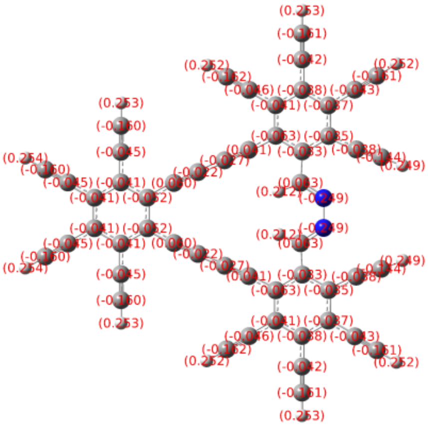

GD3d

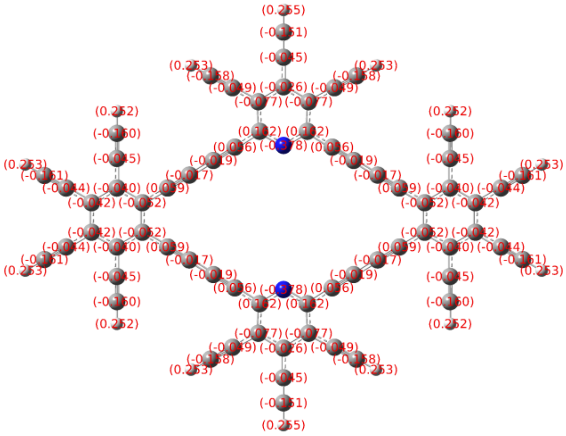

GD4d

**Fig. S9** DFT-calculated charge density distributions for the GD and N-doped GD (the model graphdiynes contain 3 or 4 units (GD3 or GD4)).

(a)

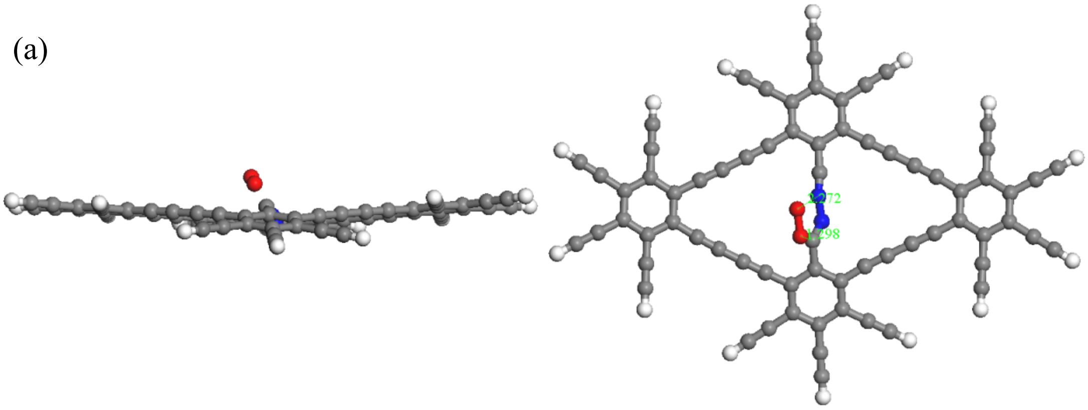

(b)

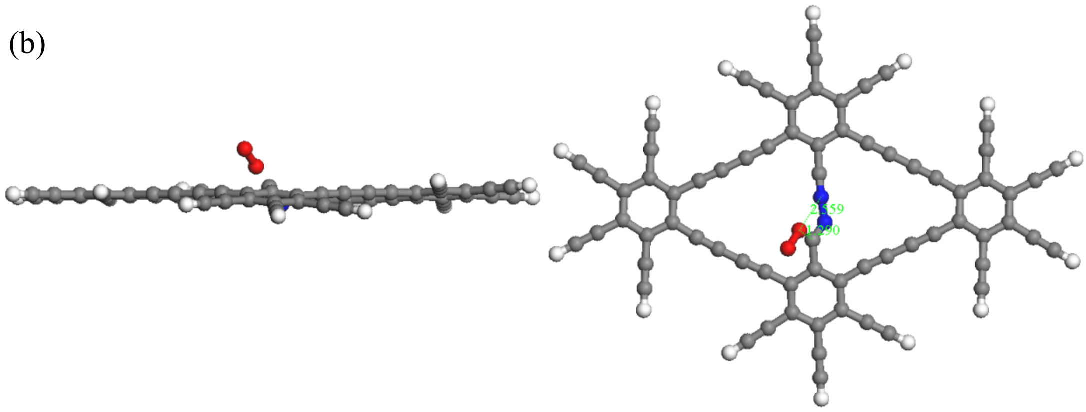

(c)

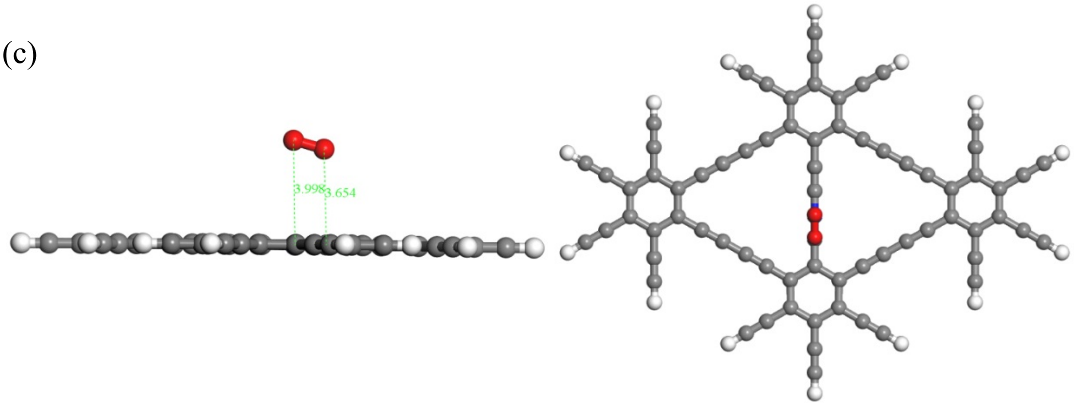

(d)

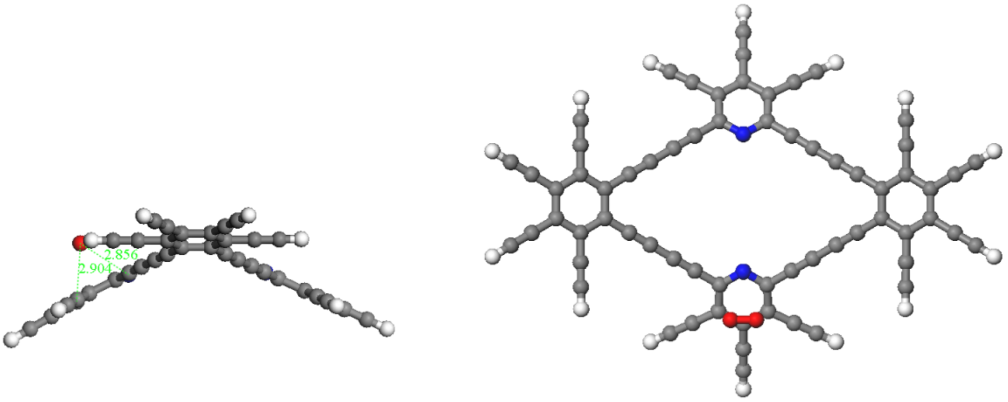

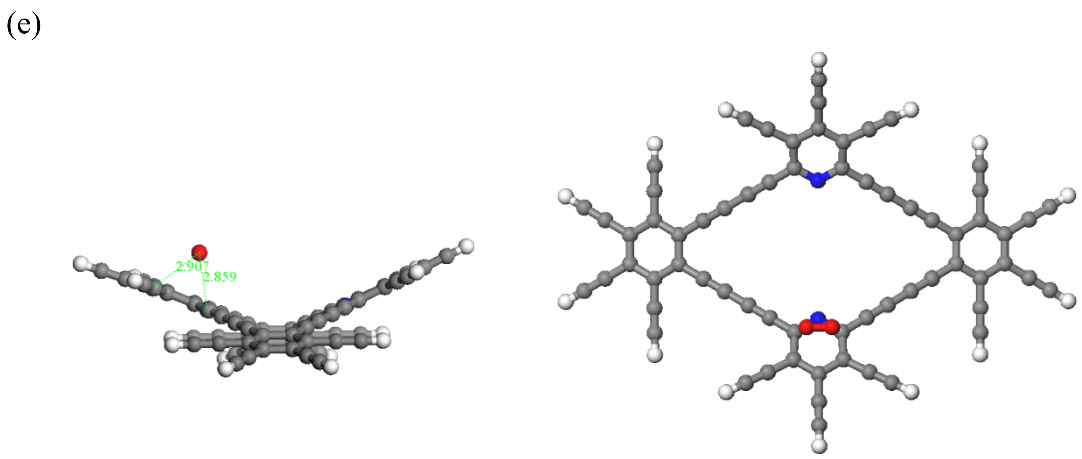

**Fig. S10** Optimized adsorption sites of $O_2$ molecule on the N-doped GD. C, O, N and H atoms are shown as gray, red, blue, and white balls. The measured distance is presented in angstrom. (a) Configuration 1 of imine N: B.E. = -101.10 kcal/mol. (b) Configuration 2 of imine N: B.E. = -95.46 kcal/mol. (c) Configuration 3 of imine N: B.E. = -29.58 kcal/mol. (d) Configuration 1 of pyridinic N: B.E. = -0.66 kcal/mol. (e) Configuration 2 of pyridinic N: B.E. = -0.43 kcal/mol.

**Table S4.** The binding energies of optimized adsorption sites of $O_2$ molecules in N-doped GD and the bond length of $O_2$ molecules in the optimized geometry.

| | B.E. (kcal/mol) | Bond length of $O_2$ molecules (Å) |
|---|---|---|
| Pure $O_2$ | | 1.210 |
| Configuration 1 of imine N | -101.10 | 1.376 |
| Configuration 2 of imine N | -95.46 | 1.372 |
| Configuration 3 of imine N | -29.58 | 1.210 |
| Configuration 1 of pyridinic N | -0.66 | 1.231 |
| Configuration 2 of pyridinic N | -0.43 | 1.231 |

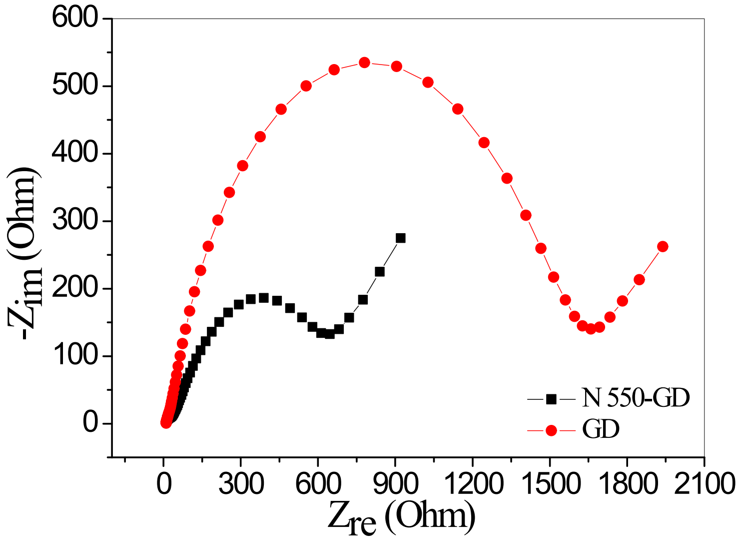

**Fig. S11** Nyquist plots of the N 550-GD and GD electrodes obtained by applying a sine wave with amplitude of 5.0 mV over the frequency range 0.01Hz–100000 Hz.